

PCCP

Accepted Manuscript



This is an *Accepted Manuscript*, which has been through the Royal Society of Chemistry peer review process and has been accepted for publication.

Accepted Manuscripts are published online shortly after acceptance, before technical editing, formatting and proof reading. Using this free service, authors can make their results available to the community, in citable form, before we publish the edited article. We will replace this *Accepted Manuscript* with the edited and formatted *Advance Article* as soon as it is available.

You can find more information about *Accepted Manuscripts* in the [Information for Authors](#).

Please note that technical editing may introduce minor changes to the text and/or graphics, which may alter content. The journal's standard [Terms & Conditions](#) and the [Ethical guidelines](#) still apply. In no event shall the Royal Society of Chemistry be held responsible for any errors or omissions in this *Accepted Manuscript* or any consequences arising from the use of any information it contains.

**Alkaline O₂ Reduction on Oxide-Derived Au:
High Activity and 4e⁻ Selectivity without (100) Facets**

Xiaoquan Min, Yihong Chen,[†] and Matthew W. Kanan*

Department of Chemistry, Stanford University, Stanford, CA 94305

[†]Current address: Applied Materials, Santa Clara, CA 95054

*Corresponding author: mkanan@stanford.edu

Abstract

Gold films produced from gold oxide precursors (“oxide-derived Au”) were compared to polyhedral Au nanoparticles for electrocatalytic alkaline O₂ reduction. Despite having no detectable abundance of (100) facets, oxide-derived Au exhibited 4e⁻ selectivity and surface-area-normalized activity that rivaled cubic Au nanoparticles with high (100) abundance. The activity of oxide-derived Au likely arises from active sites at the surface terminations of defects that are trapped during gold oxide reduction.

Introduction

Fuel cells that operate under alkaline conditions have been used in space shuttles for many years and recent developments have sparked a resurgence of interest for terrestrial applications^{1,2}. The O₂ reduction reaction (ORR) at the cathode is a principal source of efficiency losses in alkaline fuel cells. Alkaline ORR either proceeds through a 4e⁻ pathway to form HO⁻ (Eq. 1) or a 2e⁻ pathway to form HO₂⁻ (Eq. 2). To be efficient, a catalyst must have high selectivity for 4e⁻ reduction and attain maximal ORR current density with minimal overpotential. The equilibrium potential for the 4e⁻ pathway is 1.23 V vs the reversible hydrogen electrode (RHE). On most known materials, >0.4 V of overpotential is required for the onset of ORR catalysis.



Au is an exceptionally active alkaline ORR catalyst and has been studied extensively to elucidate structure–activity relationships. Single crystal electrode studies have shown large differences in ORR activity between different Au surface facets. Au(100) is the most active surface of any known material. In rotating disk electrode (RDE) voltammetry, the onset of alkaline ORR on Au(100) occurs at 1.0 V vs RHE and the half wave potential is ~0.8 V (at 1600 rpm)³. Au(100) has a high selectivity for 4e⁻ reduction in the low to moderate overpotential range. In contrast, the half wave potentials are 200 mV and 130 mV more negative on Au(111) and Au(110), respectively, and these facets favor 2e⁻ reduction⁴. High index Au facets span a range of ORR activity and selectivity, but none rivals Au(100)⁵⁻⁷.

The high activity of Au(100) terraces provides one design principle for Au nanoparticle (NP) catalysts. While Au NPs do not normally expose (100) facets because of their high surface energy, NPs with a significant fraction of (100) surface facets can be prepared by incorporating additives that bind (100) during NP synthesis^{8,9}. Previous studies have shown that these NPs have considerably higher ORR activity (per surface area) and 4e⁻ selectivity than NPs that have low (100) abundance¹⁰. While this approach is promising, the question remains whether (100) terrace is the optimal Au surface structure for ORR catalysis. The discovery of structures that are more active or more readily incorporated into NP catalysts could lead to more efficient alkaline fuel cells. Previous results provide some evidence that there are alternatives to (100). Sun et al recently reported 8 nm icosahedral Au NPs that have mostly (111) surface facets but nonetheless have an unusually high onset potential (1.0 V) and relatively high activity¹¹. These results were attributed to catalytically active defect structures at the surface terminations of twin boundaries in the NPs¹².

We recently described a material called “oxide-derived” Au (OD-Au) that is a nanocrystalline Au film produced by electrochemically reducing a Au oxide precursor¹³. OD-Au required 200 mV less overpotential than polycrystalline Au and various Au nanoparticle electrodes to selectively reduce CO₂ to

CO and suppress competitive H^+ reduction. Electrokinetic studies suggested that the improved activity on OD-Au was linked to greater stabilization of the one electron-reduced $\text{CO}_2^{\bullet-}$ intermediate on the surfaces of OD-Au. Based on these results, we hypothesized that OD-Au would have enhanced ORR activity by affording better stabilization of partially reduced intermediates. Here we describe the alkaline ORR activity of OD-Au and compare it to polyhedral Au NPs that preferentially expose different low-index facets. OD-Au exhibits ORR activity that rivals the activity of cubic Au NPs, which have one of the highest alkaline ORR activities per surface area. Whereas the activity of the cubes is associated with their high proportion of (100) surface facets, electrochemical surface analysis indicates that OD-Au does not have any significant exposure of (100). Our results provide further evidence for the presence of metastable, highly active surface structures on OD-Au that arise from defects that are kinetically trapped during the oxide reduction process.

Results and Discussion

Octahedral, dodecahedral, and cubic Au NPs were synthesized following published procedures (see Supplementary Information)^{8,9}. Scanning electron microscopy (SEM) confirmed the expected polyhedral morphology in each case (Figure 1a–c). For electrochemical measurements and ORR studies, NPs were drop-cast onto glassy carbon RDEs. OD-Au electrodes were prepared by oxidizing a Au RDE using a pulsed anodization method¹⁴ and then electrochemically reducing the oxide. The procedure was the same as used previously¹³ except that the anodization time was shortened to 5 min to prepare a thinner OD-Au layer (see the Supplementary Information). SEM of an OD-Au RDE revealed a continuous film of irregularly shaped particles ranging in size from 20 nm to 50 nm (Figure 1d). The electrochemical surface areas were measured using Cu underpotential deposition (upd). Comparable surface areas were measured for the polyhedral NPs, while OD-Au had a ~10-fold higher surface area (Table S1).

The distribution of surface facets on the polyhedral NPs and OD-Au were probed using Pb upd (Figure 1e), which identifies the low index facets of Au based on the peak potentials (E_p) of the deposition and stripping waves¹⁵⁻¹⁹. The Au octahedra exhibited a deposition wave ($E_p = -0.57$ V vs Ag/AgCl) and stripping wave ($E_p = -0.49$ V) that are characteristic of (111) facets. The Au dodecahedra exhibited a large deposition wave ($E_p = -0.45$ V) and stripping wave ($E_p = -0.31$ V) characteristic of (110), as well as a smaller pair of (111) waves. An additional broad stripping wave was observed at ~-0.58 V, which may correspond to regions of the surface with a high density of steps¹⁷. The Au cubes exhibited all of the waves seen on the octahedra and dodecahedra in addition to a deposition ($E_p = -0.54$ V) and two stripping ($E_p = -0.56$ V, -0.44 V) waves that are characteristic of (100). The magnitudes of the waves indicated an approximately even distribution of (111), (110), and (100) facets, consistent with what has been observed in previous studies of Au cubes¹⁰. The Pb upd waves for the Au polyhedral NPs provide a reference for the analysis of surface facets on OD-Au. The OD-Au electrode exhibited waves

consistent with (111) and (110) facets but no waves attributable to (100). The voltammogram resembles a combination of the Au octahedra and Au dodecahedra voltammograms with some peak shifts that may reflect smaller terraces on the OD-Au surface.

ORR electrokinetics were studied using RDE linear sweep voltammetry in 0.1 M KOH saturated with 1 atm of O₂. Figure 2a shows linear sweep voltammograms for an OD-Au electrode at various rotation rates (ω). The onset of ORR catalysis occurred at \sim 1.0 V vs RHE and the current density (j) reached a mass transport-limited plateau at 0.8 V. The data were analyzed using the Koutecky-Levich equation²⁰:

$$1/j = 1/j_k + 1/j_d$$

where j_k is the kinetic current density and j_d is the mass transport-limited current density. The inset to Figure 2a shows the Koutecky-Levich plots at potentials ranging from 0.8 V to 0.6 V. The electron transfer number (n) calculated from the slopes of the Koutecky-Levich plots was 3.95 at 0.8 V and gradually declined to 3.7 at 0.45 V (Table S2), indicating that OD-Au favors $4e^-$ reduction of O₂ to HO⁻. The kinetic current densities were determined from the intercepts of the Koutecky-Levich plots over the potential range 1.03 V to 0.83 V and divided by the electrode roughness factor to obtain the normalized j_k values. Figure 2b shows a Tafel plot of $\log(j_k)$ vs overpotential. The plot was linear from 0.28 V to 0.40 V of overpotential with a Tafel slope of 110 mV/dec. This slope is consistent with a rate-determining initial e^- transfer^{21,22} and has been observed for many Au electrodes in alkaline ORR³⁻⁵.

Figure 3 shows a comparison of ORR catalysis on OD-Au and the three polyhedral Au NPs. In linear sweep voltammetry performed at 1600 rpm, the onset potential of the cubes was comparable to OD-Au and shifted anodically by \sim 100 mV compared to the octahedra and dodecahedra (Figure 3a). The difference between the cubes and other polyhedral Au NPs reflects the higher activity of the (100) surface compared to (111) or (110). While OD-Au exhibited a much steeper increase in current than the cubes, it is difficult to compare their relative activities directly from the voltammograms because of the significantly higher surface area for OD-Au. Normalized j_k values obtained from Koutecky-Levich analysis and surface area measurements provide a better comparison. As seen in the comparison of the Tafel plots in Figure 3b, the normalized ORR activity of OD-Au is slightly greater than the Au cubes and much higher than the octahedra and dodecahedra. At 0.85 V, the most positive potential at which they can be compared directly, normalized j_k was \sim 1.4 \times higher on OD-Au compared to Au cubes and \sim 10 \times higher compared to Au octahedra and dodecahedra (Table 1). Comparison of the electron transfer numbers indicated a higher selectivity for $4e^-$ reduction on OD-Au. On Au cubes, n was close to 4 at potentials greater than 0.6 V and gradually decreased to \sim 3.4 as the potential became more negative. On Au octahedra and dodecahedra, n was 3.4–3.2, and 3.4–3.3, respectively, from 0.6 V to 0.4 V (Table 1). These values are higher than what is expected based on (111) and (110) single crystal electrodes, which

suggests that there is some HO_2^- reduction at vicinal sites on the corners and edges of octahedral and dodecahedral Au NPs.

The electrochemical surface analysis and RDE voltammetry results suggest that OD-Au has a low density of highly active catalytic sites for alkaline ORR. The Pb upd voltammograms indicate that the surfaces of OD-Au are dominated by (111) and (110) facets but the surface area-normalized activity is 10-fold higher than what is expected for these facets. While there may be small amounts of (100) facets on the surfaces of OD-Au that are not evident in the Pb upd voltammogram, their abundance would not be sufficient to account for the surface area-normalized activity, as indicated by the comparison with the Au cubes. Moreover, single crystal studies have shown that vicinal facets of Au(100), which are comprised of (100) terraces separated by steps, have substantially lower activity than Au(100), suggesting that wide terraces are required for optimal (100) activity⁵. We propose that the sites responsible for ORR on OD-Au may lie on the surface terminations of grain boundaries or linear dislocations that are kinetically trapped during reduction of Au_2O_3 to form OD-Au. Elucidating the relationship between defect surface terminations and catalytic activity may lead to new strategies for electrocatalyst design.

Acknowledgements

We thank Stanford University and the Hellman Foundation for support of this research.

References

- (1) Spendelow, J. S.; Wieckowski, A. *Physical chemistry chemical physics : PCCP* **2007**, *9*, 2654.
- (2) Park, J. S.; Park, S. H.; Yim, S. D.; Yoon, Y. G.; Lee, W. Y.; Kim, C. S. *J Power Sources* **2008**, *178*, 620.
- (3) Adzic, R. R.; Markovic, N. M.; Vesovic, V. B. *J Electroanal Chem* **1984**, *165*, 105.
- (4) Markovic, N. M.; Adzic, R. R.; Vesovic, V. B. *J Electroanal Chem* **1984**, *165*, 121.
- (5) Strbac, S.; Anastasijevic, N. A.; Adzic, R. R. *J Electroanal Chem* **1992**, *323*, 179.
- (6) Adzic, R. R.; Strbac, S.; Anastasijevic, N. *Mater Chem Phys* **1989**, *22*, 349.
- (7) Anastasijevic, N. A.; Strbac, S.; Adzic, R. R. *J Electroanal Chem* **1988**, *240*, 239.
- (8) Wu, H. L.; Kuo, C. H.; Huang, M. H. *Langmuir* **2010**, *26*, 12307.
- (9) Chung, P. J.; Lyu, L. M.; Huang, M. H. *Chem-Eur J* **2011**, *17*, 9746.
- (10) Hernandez, J.; Solla-Gullon, J.; Herrero, E.; Aldaz, A.; Feliu, J. *Journal of Physical Chemistry C* **2007**, *111*, 14078.
- (11) Lee, Y.; Loew, A.; Sun, S. H. *Chem Mater* **2010**, *22*, 755.
- (12) Petkov, V.; Lee, Y.; Sun, S.; Ren, Y. *The Journal of Physical Chemistry C* **2012**, *116*, 26668.
- (13) Chen, Y.; Li, C. W.; Kanan, M. W. *J Am Chem Soc* **2012**, *134*, 19969.
- (14) Vela, M. E.; Marchiano, S. L.; Salvarezza, R. C.; Arvia, A. J. *J Electroanal Chem* **1995**, *388*, 133.
- (15) Engelsmann, K.; Lorenz, W. J.; Schmidt, E. *J Electroanal Chem* **1980**, *114*, 11.
- (16) Engelsmann, K.; Lorenz, W. J.; Schmidt, E. *J Electroanal Chem* **1980**, *114*, 1.
- (17) Hernández, J.; Solla-Gullón, J.; Herrero, E. *J Electroanal Chem* **2004**, *574*, 185.
- (18) Hamelin, A. *J Electroanal Chem* **1984**, *165*, 167.
- (19) Hamelin, A.; Lipkowski, J. *J Electroanal Chem* **1984**, *171*, 317.
- (20) Bard, A. J.; Faulkner, L. R. *Electrochemical Methods: Fundamentals and Applications*; John Wiley & Sons: New York, 2001.
- (21) Schmidt, T. J.; Stamenkovic, V.; Arenz, M.; Markovic, N. M.; Ross, P. N. *Electrochim Acta* **2002**, *47*, 3765.

(22) Blizanac, B. B.; Ross, P. N.; Markovic, N. M. *J Phys Chem B* **2006**, *110*, 4735.

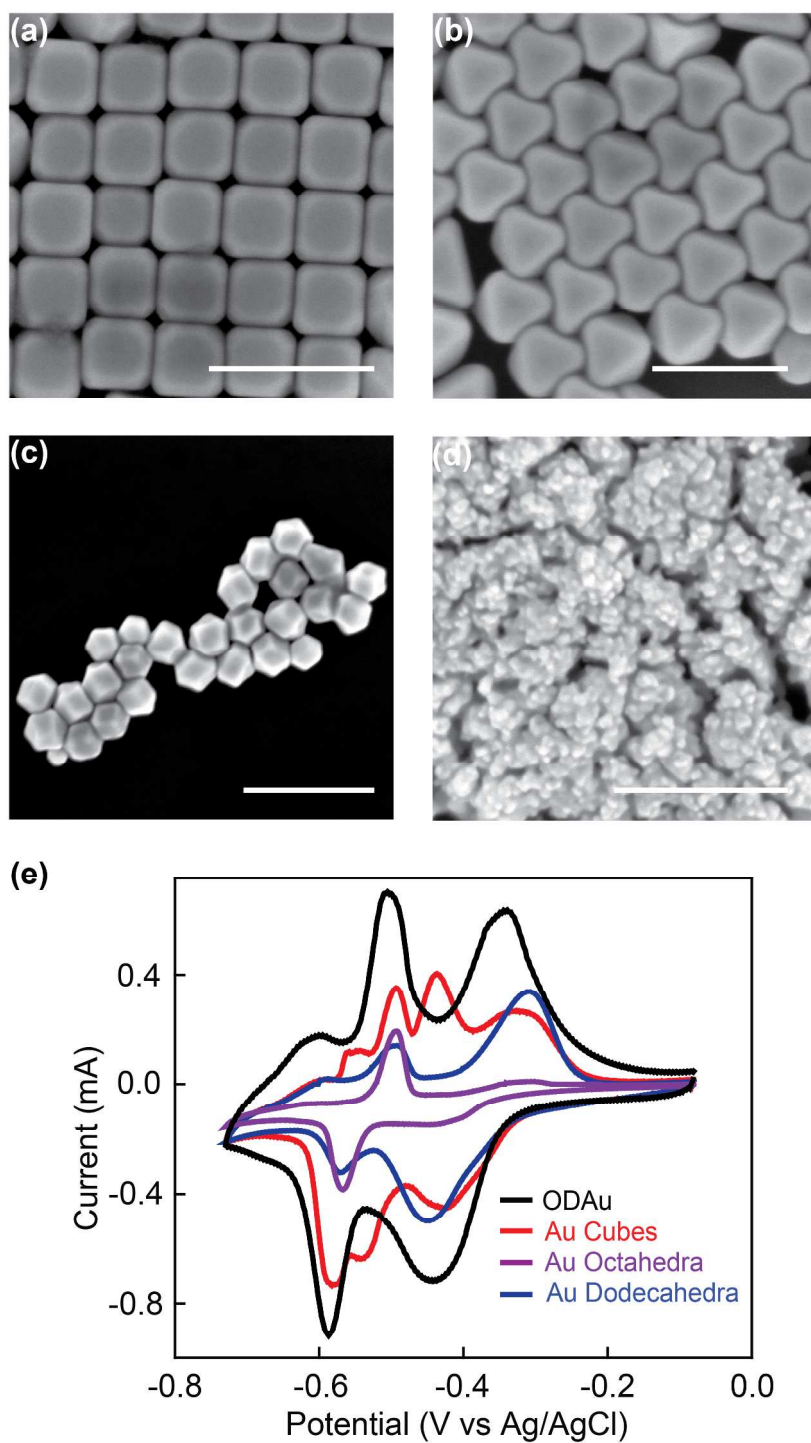


Figure 1: SEM images of (a) Au cubes, (b) Au octahedra, (c) Au dodecahedra, and (d) OD-Au. All scale bars are 200 nm. (e) Pb-upd profiles of OD-Au and shaped Au nanoparticles in 0.1 M NaOH with 1 mM $\text{Pb}(\text{CH}_3\text{COO})_2$. Scan rate: 50 mV/s.

Figure 2

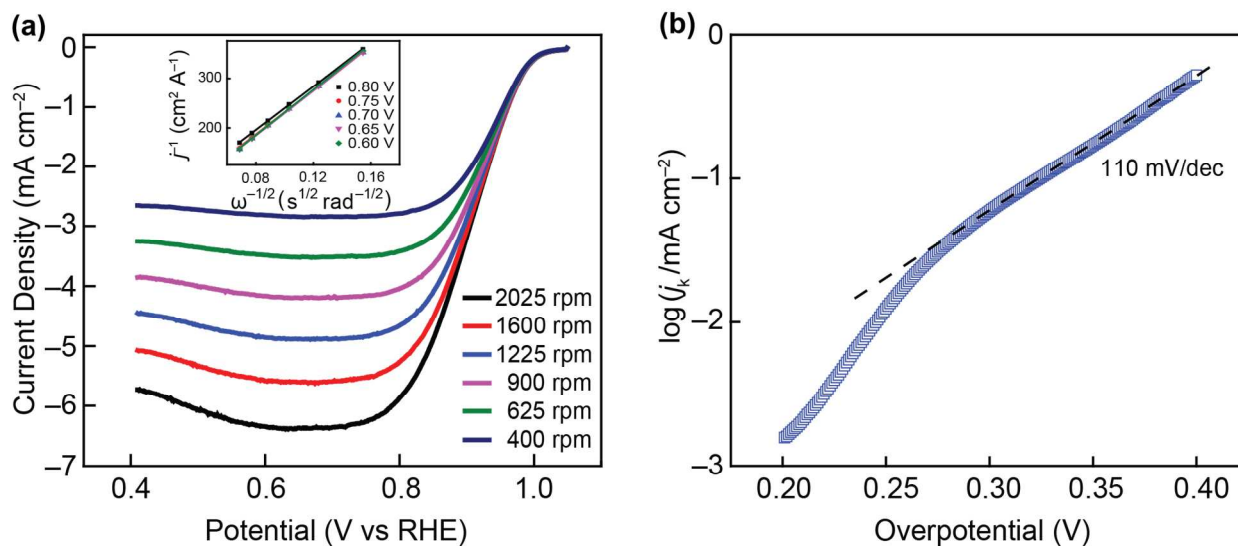


Figure 2: (a) Rotating-disk voltammograms of OD-Au in O_2 -saturated 0.1 M KOH at different rotation rates with a scan rate of 10 mV/s. The inset shows the corresponding Koutecky-Levich plots at different potentials. (b) Tafel plot of OD-Au derived from the RDE data using Koutecky-Levich equation. j_k values is the surface-area-normalized kinetic current density.

Figure 3

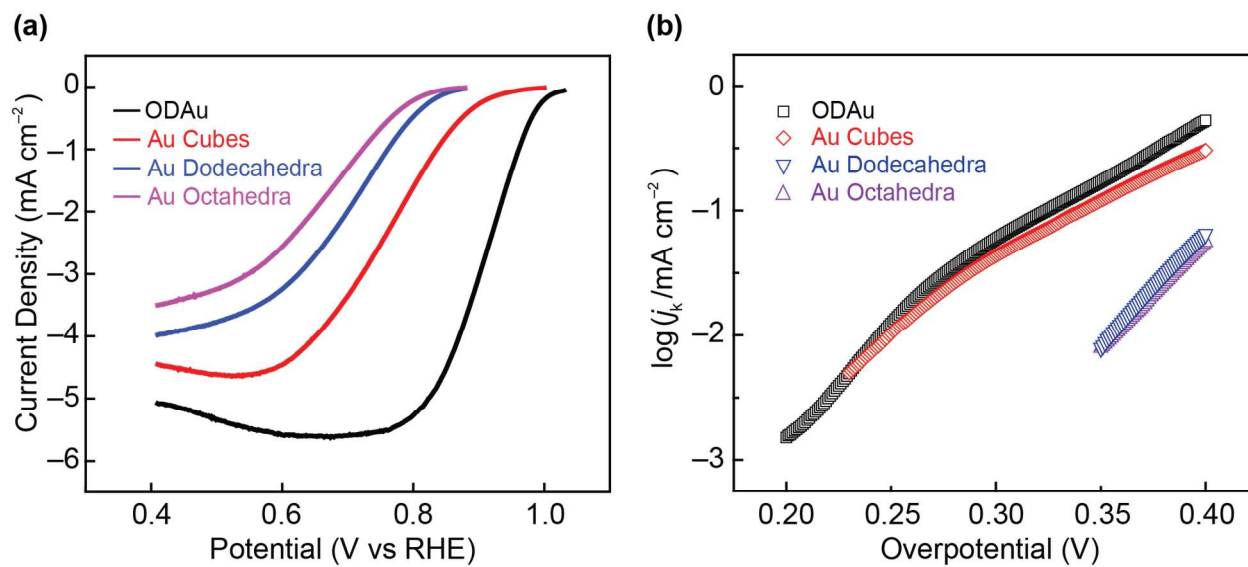


Figure 3: ORR activity comparison between OD-Au and shaped Au nanoparticles in O₂-saturated 0.1 M KOH. (a) RDE voltammograms at 1600 rpm with a scan rate of 10 mV/s; (b) Tafel plots. j_k is the surface-area-normalized kinetic current density.

Table 1

	Onset Potential (V vs RHE)	n	j_k at 0.9 V vs RHE (mA cm ⁻²)	j_k at 0.85 V vs RHE (mA cm ⁻²)
OD-Au	~1.03	3.95–3.7	0.11	0.33
Au Cubes	~1.0	4.0–3.4	0.086	0.23
Au Octahedra	~0.88	3.4–3.3	-	0.033
Au Dodecahedra	~0.88	3.4–3.2	-	0.028

Table 1: ORR activity comparison between OD-Au and shaped Au nanoparticles. The n values were calculated from the slopes of the Koutecky-Levich plots over 0.8 V to 0.45 V (OD-Au), 0.8 V to 0.4 V (cubes), and 0.6 V to 0.4 V (octahedra and dodecahedra).